

## Cosmic Ray Antiproton Observations From 0.2 To 3.2 GeV

A.W. Labrador<sup>1</sup>, W. Menn<sup>3</sup>, L.M. Barbier<sup>2</sup>, E.R. Christian<sup>2</sup>, A.J. Davis<sup>1</sup>,  
R.L. Golden<sup>4</sup>, M. Hof<sup>3</sup>, K.E. Krombel<sup>2</sup>, R.A. Mewaldt<sup>1</sup>, J.W. Mitchell<sup>2</sup>, J.F. Ormes<sup>2</sup>,  
O. Reimer<sup>3</sup>, S.M. Schindler<sup>1</sup>, M. Simon<sup>3</sup>, S.J. Stochaj<sup>4</sup>, R.E. Streitmatter<sup>2</sup>,  
I.L. Rasmussen<sup>5</sup>, and W.R. Webber<sup>4</sup>

<sup>1</sup>California Institute of Technology, Pasadena, CA 91125, USA

<sup>2</sup>NASA/Goddard Space Flight Center, Greenbelt, MD 20771, USA

<sup>3</sup>University of Siegen, 57068 Siegen, Germany

<sup>4</sup>New Mexico State University, Las Cruces, NM 88003, USA

<sup>5</sup>Danish Space Research Institute, Lyngby, Denmark

### Abstract

The Isotope Matter Antimatter Experiment (IMAX) has detected 16 antiprotons, in the energy range from 0.2 to 3.2 GeV. This result provides significant improvement in statistical accuracy over previous cosmic ray antiproton measurements in the same energy range. This measurement has been corrected for instrumental and atmospheric losses, yielding top-of-the-atmosphere antiproton to proton ratios in three energy intervals. These results are consistent with recent theoretical predictions in which antiprotons are produced as secondary cosmic rays and are transported through the galaxy according to the standard Leaky Box model.

### 1. Antiprotons at the Instrument

The Isotope Matter Antimatter Experiment (IMAX) and its payload performance during the flight of 16 July 1992, from Lynn Lake, Canada, have been described previously [1]. The data analysis and selection criteria for identifying antiprotons in flight data are described in a separate paper in these proceedings [2]. The resulting measurements at the instrument are summarized in Table 1.

TABLE 1: IMAX Results, at the Instrument

Energy (GeV)	# Protons	# Antiprotons
0.2 — 1.0	$1.38 \times 10^5$	3
1.0 — 2.6	$1.36 \times 10^5$	8
2.6 — 3.2	$2.3 \times 10^4$	5

Energy bins are defined by measured velocities. The protons and antiprotons in the two lower energy bins were mass-resolved via the TOF-Rigidity technique. The Cherenkov-Rigidity technique, employing two aerogel Cherenkov counters ( $n \approx 1.043$ ), was used to identify particles in the highest energy bin, with the 2.6 GeV threshold being defined as 16% of the Cherenkov light yield for a  $Z=1$ ,  $\beta=1$  particle. The 3.2 GeV upper limit corresponds to 36% of the light yield for a  $Z=1$ ,  $\beta=1$  particle.

## 2. Instrumental and Atmospheric Corrections

Comparison of the IMAX antiproton measurements with theoretical predictions requires that atmospheric and instrumental production and loss be taken into account. Primary protons and antiprotons detected by IMAX had to pass through  $\sim 5 \text{ g/cm}^2$  of residual atmosphere above the payload. Furthermore, the instrument trigger required that the particles had to pass through  $\sim 20 \text{ g/cm}^2$  of instrument material — primarily aluminum, Teflon, scintillator plastics, and silica aerogel. Additionally, account must be taken of instrumental effects such as photoelectron statistical fluctuations and detector inefficiencies.

### 2.1 Instrumental Corrections

Fluctuation in aerogel Cherenkov light yields provides a possible source of instrumental background and detector inefficiency in the highest energy bin. At magnetic rigidities ( $R=pc/Ze$ ) below  $\sim 4 \text{ GV}$ , antiprotons travel slow enough that their Cherenkov signals are low or negligible, while electrons, muons, and pions of the same magnetic rigidity travel fast enough that their average light yields approach the maximum yield for  $Z=1, \beta=1$  particles.

However, Poisson fluctuations in the Cherenkov light yields, knock-on electron contributions, residual uncertainties in Cherenkov response maps and indexes, and PMT dynode statistics may fluctuate an antiproton light yield sufficiently high enough to throw it out of the selected light yield range. Similarly, electron, muon, and pion signals may fluctuate low enough to simulate antiproton light yields. Monte Carlo simulations of IMAX measurements show that, for the 2.6–3.2 GeV energy range, electron/muon/pion light yield fluctuations may produce approximately 1 false antiproton. In the lower energy bins, the time-of-flight (TOF) system combines with the Cherenkov counters to eliminate essentially all such background.

With  $\sim 20 \text{ g/cm}^2$  of instrument material, annihilation will be the primary loss mechanism for antiprotons. Geometric arguments show that almost all annihilation events in the instrument will be rejected in data analysis, and similar arguments show that most antiproton and proton secondaries produced in the instrument will also be rejected. To calculate correction factors for annihilation, we use an energy-dependent cross section,  $\sigma(\text{annihil}) = 42.0 \times (E^{-0.43} - 0.476) \text{ mb}$ , for antiproton annihilation on protons [3], where energy is in GeV. We scale cross sections by  $\sim \pi(0.55 \times 10^{-13} + 1.29 \times 10^{-13} A^{1/3})^2 \text{ cm}^2$  to the various materials in IMAX, normalized to annihilation cross section data [4]. From this scaling, we calculate the correction factors for antiproton losses to be 1.40, 1.20, and 1.16, averaged over each energy bin, from the low energy bin to the high energy bin. Finally, we estimate a correction factor of 1.04 for antiproton events which annihilate below the instrument. This factor applies only to the 0.2–1 GeV energy bin.

### 2.2 Atmospheric Corrections

Given the relatively high energies and wide energy bins, proton energy loss can largely be ignored. The remaining correction to the proton measurement arises from production of secondary atmospheric protons, for which we use a calculation by Papini, et al. [5]. We normalize these calculations to 1992 solar modulation levels and  $\sim 5 \text{ g/cm}^2$  of atmosphere, and the resulting ratios of secondary atmospheric protons to primary protons are 0.244, 0.048, and 0.035, from the low energy bin to the high energy bin. We apply a similar normalization to a calculation by Stephens [6] to estimate the number of secondary atmospheric antiprotons. We find that approximately 2.5 antiprotons detected by IMAX

may be due to secondary atmospheric production. Most of these secondary atmospheric antiprotons occupy the 1.0–2.6 GeV energy bin. Cross sections for annihilation of antiprotons in the atmosphere are calculated in the same way as in the instrument. The resulting correction factors are 1.09, 1.05, and 1.04, from the lowest energy bin to the highest.

Finally, the top of the atmosphere IMAX antiproton to proton ratios are given in Table 2. Uncertainties are calculated for only the antiproton counting statistics.

TABLE 2: IMAX Antiproton/Proton Ratios

Energy (GeV)	Antiproton/Proton ratio
0.2 — 1.0	$4.0 (+4.2, -2.4) \times 10^{-5}$
1.0 — 2.6	$6.4 (+3.8, -2.7) \times 10^{-5}$
2.6 — 3.2	$1.9 (+1.8, -1.2) \times 10^{-4}$

### 3. Comparison of IMAX Results with Theoretical Predictions

For comparison with theoretical models, we use the interstellar proton and antiproton spectra calculated by Webber and Potgieter (hereinafter W&P) [7]. We use a spherically-symmetric solar modulation model [8] to modulate the W&P interstellar proton spectrum to coincide with the 121–230 MeV proton flux measured by IMP-8 at the time of the IMAX flight [9]. The required modulation parameter is  $\phi=749$  MV. Similarly, we modulate the

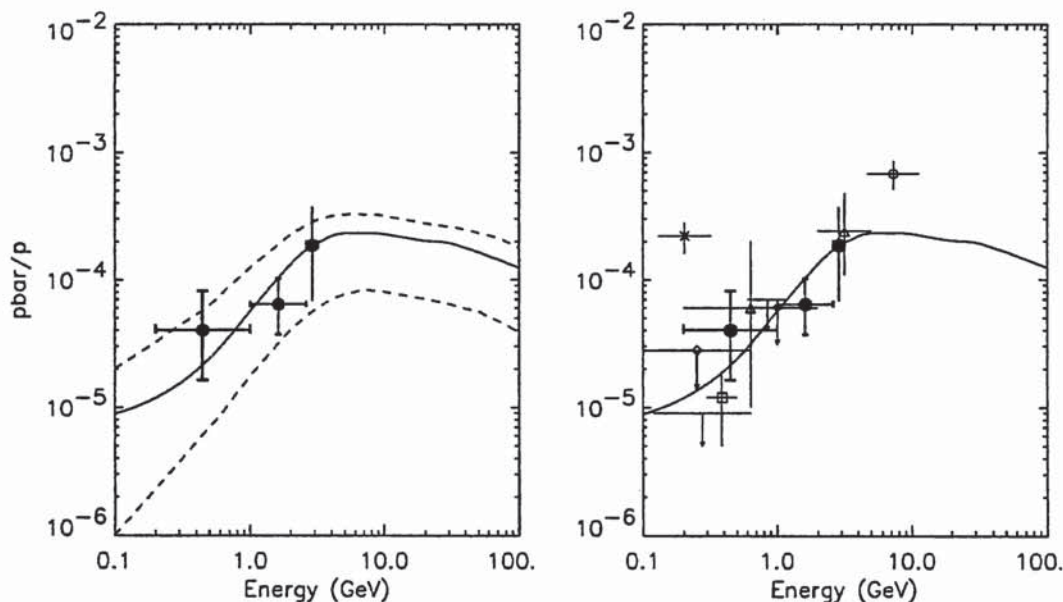


Figure 1: (a) Comparison of the IMAX antiproton/proton ratios with the calculated ratio obtained by modulating the W&P [7] interstellar spectra to 1992 levels (solid line) and with the extrema calculated by G&S [10]; (b) comparison with previous measurements. The points are IMAX (bold, filled circles), Golden, et al [11] (open circle), Bogomolov, et al. [12] (open triangles), Buffington, et al. [13] (asterisk), Stochaj [14] (no symbol), Salamon et al. [15] (open diamonds), and Yoshimura, et al. [16] (open square).

W&P interstellar antiproton flux with the same modulation parameters. Our solar modulation model assumes no charge sign dependence. In their paper, Webber and Potgieter [7] have considered possible charge sign dependent modulation effects.

Figure 1 shows the antiproton to proton ratio calculated for 1992 from the proton and antiproton spectra. The IMAX data points are also shown in Figure 1a, and the points generally lie within one sigma of the calculated ratio. For comparison with another calculation, Figure 1a includes the limits on the antiproton to proton ratio calculated by Gaisser and Schaeffer [10]. The IMAX data points lie well within those extrema. For comparison with previous measurements, Figure 1b includes data from Golden, et al. [11], Bogomolov, et al. [12], Buffington et al. [13], Stochaj [14], Salamon, et al. [15], and Yoshimura, et al. [16]. It should be noted that the theoretical curve as shown is applicable only to the 1992 solar modulation levels. The effects of solar modulation on the low energy antiproton to proton ratio over the course of the solar cycle are discussed elsewhere in these proceedings [17].

#### 4. Conclusions

The IMAX points clearly show the expected decrease, due to kinematics, in the antiproton to proton ratio at low energies. Furthermore, the points give significantly improved statistical accuracy over previous measurements in the same energy ranges. The IMAX data points agree, to within measurement uncertainties, with predictions derived from standard cosmic ray transport models in which antiprotons originate solely as secondaries.

#### Acknowledgements

This research was supported in part by NASA grant NAGW-1919. One of us (AWL) thanks the NASA Graduate Student Researchers Program for its support. The IMAX team is grateful to the NSBF for a successful balloon flight.

#### References

- [1] Mitchell, J.W. et al., Proc. 23rd Intl. Cosmic Ray Conf., Calgary. **1**, 519 (1993).
- [2] Mitchell, J.W. et al., these proceedings.
- [3] Flaminio, V., et al., CERN-HERA Report No. 84-01 (1984).
- [4] Agnew, L.E., et al., Phys. Rev., **108**, 1545 (1957).
- [5] Papini, P., Grimani, C., and Stephens, S.A., Proc. 23rd Intl. Cosmic Ray Conf., Calgary. **3**, 761 (1993).
- [6] Stephens, S.A., Proc. 23rd Intl. Cosmic Ray Conf., Calgary. **2**, 144 (1993).
- [7] Webber, W.R., and Potgieter, M.S., Ap. J., **344**, 779 (1989).
- [8] Fisk, L.A. Journal of Geophysical Research, **76**, 221 (1971).
- [9] McGuire, W., Schuster, P., and McDonald, F. Private communication.
- [10] Gaisser, T.K., and Schaeffer, R.K., Ap. J., **394**, 174 (1992).
- [11] Golden, R.L., et al. Astrophysical Letters, **24**, 75 (1984).
- [12] Bogomolov, E.A., et al. Proc. 20th Intl. Cosmic Ray Conf., Moscow, **2**, 72 (1987). Bogomolov, E. A., et al. Proc. 21st Intl. Cosmic Ray Conf., Adelaide, **3**, 288 (1990).
- [13] Buffington, A., Schindler, S.M., and Pennypacker, C.R. Ap. J., **248**, 1179 (1981).
- [14] Stochaj, S.J., Ph.D. Thesis of U. of Maryland, (1990). Also Moats, A. et al., Proc. 21st Intl. Cosmic Ray Conf., Adelaide. **3**, 284 (1990).
- [15] Salamon, M.H., et al. Ap. J., **349**, 78 (1990).
- [16] Yoshimura, K., et al. KEK Preprint 94-202. Submitted to Phys. Rev. Letters, March 1995.
- [17] Labrador, A.W., and Mewaldt, R.A., these proceedings.